

## STM Study of CO and NO on Pt(001)

M.-B. Song,<sup>\*</sup> K. Momoi,<sup>†</sup> C.-W. Lee,<sup>‡</sup> and M. Ito<sup>‡</sup>

*Institute of Science and Technology, Korea University, Chochiwon, Chungnam 339-700, Korea*

*<sup>\*</sup>Department of Chemistry, Keio University, Hiyoshi, Kohoku-Ku, Yokohama 223-8522, Japan*

*<sup>‡</sup>Department of Chemistry, Korea University, Chochiwon, Chungnam 339-700, Korea*

*Received February 10, 2000*

Adsorption of CO and NO molecules on a Pt(001)-hex R0.7° surface at 90 K is investigated by scanning tunneling microscopy (STM) in ultra-high vacuum environments. At an initial stage of adsorption, both molecules are preferentially adsorbed on the less coordinated Pt atoms of the surface with hexagonal structure, which act as active sites. Domains of the adsorbates grow parallel to the stripe structure of the reconstructed surface because of lower migration energy in this direction. The extra Pt atoms produced from adsorbate-induced restructuring give rise to anisotropic islands on the (1 × 1) surface. Each of the adsorbed NO molecules at low coverages is atomically resolved during STM observation. However, the spots of the adsorbed CO are invisible. Such a behavior is probably explained in terms of different interactions between the adsorbates.

### Introduction

Surface processes of carbon monoxide (CO) and nitrogen monoxide (NO) gases on platinum metal surfaces are of interest and importance in surface chemistry related to the area of air pollution control as well as in fundamental surface science. The adsorption of molecules is one of the most elementary surface processes. A variety of interesting adsorption processes originate from the geometric properties of metal surfaces. Particularly, the (001) surface among the low index surfaces for a fcc Pt crystal has received considerable attention from several aspects. A clean Pt(001) surface is reconstructed to show a  $\begin{pmatrix} 14 & 1 \\ -1 & 3 \end{pmatrix}$  structure (or Pt(001)-hex R0.7° structure), so called a hexagonal structure.<sup>1-4</sup> Its detailed structure will be presented later. Therefore, the atoms of the reconstructed (001) surface has a variety of the coordination number with the atoms of the second layer due to mismatching between the topmost layer (with hexagonal structure) and the second top (1 × 1) layer.

Adsorption of CO<sup>2,3,5-15</sup> and NO<sup>4,13-19</sup> on a Pt(001) substrate has been extensively studied by use of low energy electron diffraction (LEED), photoelectron spectroscopy (PES), electron energy loss spectroscopy (EELS), thermal desorption spectroscopy (TDS), infrared reflection absorption spectroscopy (IRAS), calorimetry, work function measurement, Rutherford backscattering, molecular beam scattering, and scanning tunneling microscopy (STM). However, most works have been concerned with a phase transition from a hexagonal structure to a (1 × 1) structure, induced by CO or NO adsorptions. The initial adsorption states of molecules on a Pt (001) surface has hardly been studied, despite the fact that the adsorption states have important information about the interactions of gases with substrates as well as between adsorbates.

STM has been extensively used to determine detailed structure of adlayers chemisorbed on metal surfaces with atomic resolution, although adsorbed molecules were sometimes distorted or even invisible in STM images, due to the electric field by the tip on an adspecies, surface migration,

and the frustrated translations or rotations of an adsorbate.<sup>20</sup> In this article, we describe STM observation of the CO or NO-covered Pt(001) surfaces at 90 K in UHV environments.

### Experimental Section

The apparatus and the sample preparation procedure have been described elsewhere.<sup>3,18</sup> The experiments were carried out in an ultra-high vacuum chamber with a base pressure of  $1 \times 10^{-8}$  Pa. The system was equipped with a reflection high-energy electron diffractometer (RHEED), a quadrupole mass spectrometer, a variable leak valve and STM (JEOL, JSTM-4610) in the STM observation chamber, as well as an Ar<sup>+</sup> ion sputtering gun and an O<sub>2</sub> gas variable leak valve in the sample treat chamber. All STM images presented here were obtained in a constant height mode using tungsten tips. The tip was prepared by electrochemical etching of a tungsten wire with a diameter of 3 mm at 10 V dc in a 2 N NaOH solution, and was cleaned by heating in a vacuum and by field evaporation while tunneling. The bias voltage was referred to the sample voltage with respect to the tip.

The single crystal Pt(001) sample was oriented to within 1° accuracy by using the Laue method and was polished using conventional metallographic technique. It was approximately 5 × 5 mm<sup>2</sup> in square and 1 mm thick. The sample was able to be heated with an electron beam heater and was cooled to 90 K by filling a cryostat with liquid nitrogen. The Pt sample surface was cleaned by repeated cycles of Ar<sup>+</sup> ion sputtering, annealing in the presence of oxygen of  $2 \times 10^{-5}$  Pa and flashing for 60 seconds. The cleanliness and order of the surface were checked by RHEED and STM. CO and NO gases were introduced into the chamber by means of the gas variable leak valve. CO and NO molecules were non-dissociatively adsorbed on a clean Pt(001)-hex R0.7° surface

### Results and Discussion

**CO adsorption.** A clean, hexagonally reconstructed Pt(001)

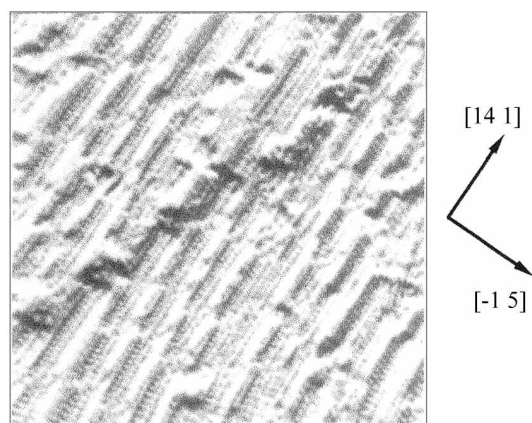


**Figure 1.** STM image of CO molecules adsorbed on a Pt(001)-hex R0.7° surface after CO exposure of 1 L at 90 K ( $17.3 \times 17.3 \text{ nm}^2$ ). Tunneling condition: sample bias voltage =  $-0.036 \text{ V}$  and tunneling current =  $1.78 \text{ nA}$ .

surface with a single domain was observed over wider regions than  $100 \times 100 \text{ nm}^2$  area.<sup>3</sup> After exposing the Pt surface to CO gas of 1 L at 90 K, we obtained an STM image of the CO-covered Pt(001) surface, shown in Figure 1. Bright (corresponding to higher tunneling currents), narrow domains associated with CO adsorption run parallel with the reconstructed stripe (the [14 1] direction of longer periodicity of the hexagonally reconstructed surface). Distance between the domains along the [-1 5] direction was mainly 5a or 10a, where a is the length of a Pt(001)-(1 × 1) surface unit cell. Each of Pt substrate atoms between the bright domains is clearly visible on the atomically resolved STM image and has still remained the hexagonal structure. The result indicates that CO-induced lifting of hex-R0.7° phase to (1 × 1) phase does not occur at all, under such a low coverage. This agrees with the previous IRAS study.<sup>8</sup> Therefore, the bright domains represent clusters of the adsorbed CO molecules rather than Pt atoms. CO molecules inside the domains are not able to be atomically resolved due to a fast migration.<sup>2,21,22</sup> However, appearance of an anisotropic shape of the CO clusters seems to reflect an anisotropic diffusion. The diffusion rate is fast due to low corrugation of the [14 1] direction as compared with the [-1 5] direction of shorter periodicity, as previously observed in Au/Au(001), Pt/Pt(001), NO/Pt(001) (present paper) and Sm/Pt(001) systems.<sup>1,4,23,24</sup>

Figure 2(a) shows an STM image taken after an amount of CO exposure was increased to 4 L. The image is divided into three different areas as regions (I), (II) and (III), depending on the coverage of adsorbed CO molecules. Stripe structures have still remained on regions of (I) and (II). A current vs. distance curve along the line (marked by the white line) perpendicular to the direction of the two stripes is plotted out in Figure 2(b). A model of hexagonal structure of a clean Pt(001) surface is shown in Figure 2(c).<sup>1-4</sup> The right part of Figure 2(c) displays cross-section along the two arrows. Solid and open circles indicate Pt atoms in the topmost (hex) surface and in the second (1 × 1) layer, respectively. The three surface atoms in (A) of Figure 2(c) locate right above the second top layer atoms, whereas those in (B) in between

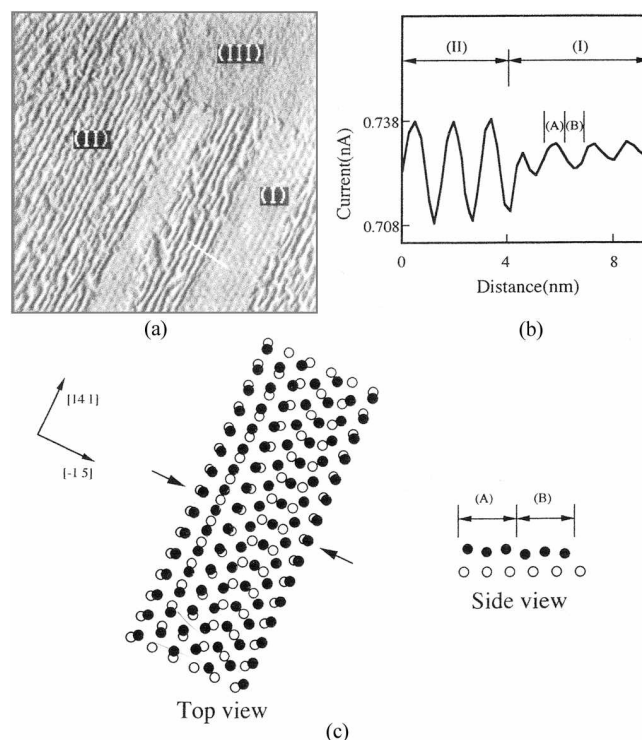


**Figure 2.** (a) STM image of CO adsorbed on Pt(001) taken after CO exposure of 4 L at 90 K ( $45.4 \times 45.4 \text{ nm}^2$ ). Tunneling condition: sample bias voltage =  $0.013 \text{ V}$  and tunneling current =  $0.81 \text{ nA}$ . (b) Current vs. distance curve along the solid line in Figure 2(a). (c) A model of hexagonal structure of a clean, reconstructed Pt(001) surface. Solid and open circles indicate atoms in the topmost (hex) surface and the second top (1 × 1) layer, respectively.

second layer atoms. Therefore, an STM image for the clean Pt(001) surface having hexagonal structure exhibits stripe structures, in which the regions of (A) and (B) are observed as brighter and darker rows, respectively. The stripe structure that is observed in the region (I) shows a bare, reconstructed surface, since the image of the region (I) was identical with an STM image of a clean Pt(001)-hex R0.7° surface.<sup>3</sup> However, the possibility for a CO-covered surface with an extremely low coverage can not be ruled out because a rapid migration of CO molecules over the surface made difficult to detect CO molecules.

The other stripe structure can be observed in the region (II) in Figure 2(a). Comparing two stripe structures in (I) and (II) regions, we can derive the followings from the current vs. distance curve of Figure 2(b): (1) The corrugation of the stripe of the region (II) is much larger than that of the region (I) of the clean surface. (2) There is no phase difference in the corrugation between the regions of (I) and (II). (3) Distances between bright rows are equal to 5a on both regions. The three facts reveal that at an initial stage of adsorption CO molecules are preferentially adsorbed on the surface Pt atoms of the region (A) shown in Figure 2(c). In this respect, we recall the result of Wandelt's local work function,<sup>25</sup> that an adsorbed CO molecule is strongly bound to an active step site (or other defect sites). This means that the surface atoms in (A) are able to act as active sites because these are less

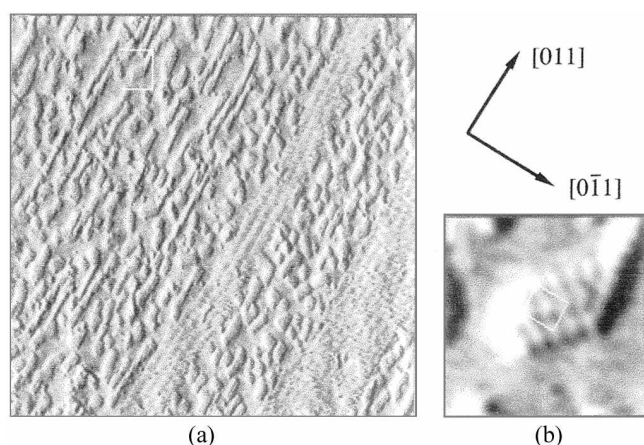


**Figure 3.** (a) STM image obtained at a sample temperature of 90 K after annealing the surface of Figure 2(a) up to 200 K ( $45.2 \times 45.2 \text{ nm}^2$ ). (b) An enlarged STM image of the square area in Figure 3(a) ( $3.65 \times 3.65 \text{ nm}^2$ ). Tunneling condition: sample bias voltage = 0.048 V and tunneling current = 1.20 nA.

coordinated than in (B).

The image of the region (III) is not clear but our zoom-out image<sup>3</sup> displays that the lifting of a hexagonal surface to a flat ( $1 \times 1$ ) surface is induced by CO adsorption. The adsorbed CO molecules give rise to a  $c(\sqrt{2} \times \sqrt{2})R45^\circ$  structure with a coverage of 0.67.<sup>3</sup>

Figure 3(a) shows an STM image obtained at 90 K but after heating the surface (the two regions of (I) and (II)) of Figure 2(a) up to 200 K. The stripe structure that was observed in the region (I) of Figure 2(a) has still remained unchanged. The result reveals that structural change has not occurred on the bare surface even after heating. On the contrary, the CO-covered region (II) of Figure 2(a) was restructured to a ( $1 \times 1$ ) phase having flat structure. In addition, a large number of clusters were observed on the flat surface. On a closer inspection, there are two kinds of clusters on the ( $1 \times 1$ ) surface; one is an elongated cluster along the  $[14\ 1]$  direction (or  $[011]$  direction) and the other is relatively an isotropic one. Figure 3(b) displays the expanded STM image for the square area (corresponding to the latter cluster) in Figure 3(a). The CO molecules have a  $(\sqrt{2} \times \sqrt{2})R45^\circ$  (or  $c(2 \times 2)$ ) superstructure rotated by  $45^\circ$  from the  $[011]$  direction, with a coverage of 0.5. The structure was previously observed by LEED.<sup>6</sup> The former (elongated cluster) is probably attributed to the islands formed by the 'extra' Pt atoms, since the distances between the nearest neighbor spots are about  $a$ . The presence of the extra Pt atoms can be explained by the difference of the Pt atom surface density. The Pt atom density of the hexagonal surface is larger (approximately 25%) than that of the ( $1 \times 1$ ) surface.<sup>16</sup> As a result, the extra Pt atoms were produced on the flat surface because of the restructuring of the hex surface to due to the ( $1 \times 1$ ) surface.

**NO adsorption.** Figure 4(a) and 4(b) show STM images of NO-covered Pt(001) surface after low (0.8 L) and higher (2 L) exposures of NO at 90 K, respectively. At the low coverage, the stripe structure indicating the bare, reconstructed surface with a width of  $5a$  was also observed over the wide

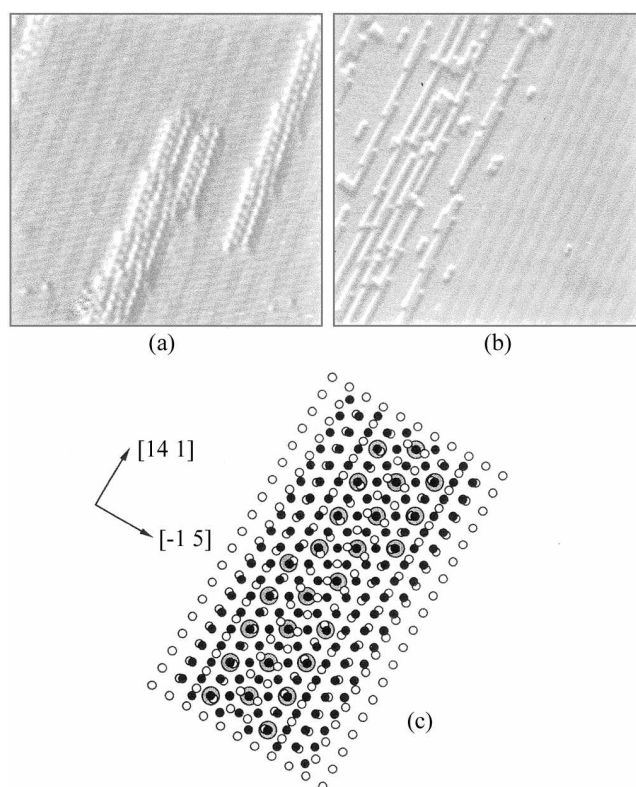


**Figure 4.** STM images of NO-covered Pt(001) surface at (a) low and (b) higher exposures of NO at 90 K. Tunneling conditions for (a) and (b) with image sizes of ( $13.9 \times 13.9 \text{ nm}^2$ ) and ( $18.0 \times 18.0 \text{ nm}^2$ ); sample bias voltage = 0.277 and 0.007 V, and tunneling current = 4.18 and 4.37 nA, respectively. (c) A structural model of the NO molecules on the Pt(001)-hex  $R0.7^\circ$  surface. NO admolecules are shown as large shaded circles, small solid and open circles indicate reconstructed first-layer atoms and second-layer atoms of Pt substrate, respectively.

region of Figure 4(a). NO-covered domains, which exhibited much higher tunneling currents, on the hexagonal surface were obtained at the center and the right parts of Figure 4(a). During NO adsorption, the adsorbed NO molecules formed a two-dimensional structure, of which the NO domains contain mainly seven (parallel to the  $[14\ 1]$  direction) and three molecules (the  $[-1\ 5]$  direction), corresponding to the size of the unit cell of a Pt(001)-hex  $R0.7^\circ$  surface. Such a two-dimensional structure appears to strongly reflect the reconstructed surface. Measuring the distance from the stripe structure of the bare surface along the  $[-1\ 5]$  direction, these three NO molecules are assignable to the molecules bound to the surface Pt atoms locating on-top and bridging sites on the second top layer. The reason why NO molecules are selectively adsorbed on the low-coordinated Pt atoms is similar to the case of the CO adsorption. A structural model corresponding to the two-dimensional structure is shown in Figure 4(c). The NO admolecules are shown as large shaded circles, small solid and open circles indicate reconstructed first-layer atoms and second-layer atoms of Pt substrate, respectively. The adsorbed NO molecules give a structure of  $p(2 \times 2)$  or quasi- $c(4 \times 2)$  with respect to the hexagonal or the ( $1 \times 1$ ) surfaces, respectively.<sup>18</sup> The fact that a  $p(2 \times 2)$

structure of NO was observed on the hex-Pt(001) surface having a hexagonal structure is in accord with a previous LEED result that the adsorption structure of NO on a Pt(111) surface was  $p(2 \times 2)$  at saturation ( $\theta = 0.25$ ).<sup>26</sup>

At the high exposure, the symmetry of an NO-covered surface is changed to a flat ( $1 \times 1$ ) surface as shown at the left part of Figure 4(b). In addition, the flat islands (formed by the extra Pt atoms) having monatomic height on a flat ( $1 \times 1$ ) surface were observed. A simple  $c(4 \times 2)$ -NO structure with a saturation coverage of 0.25 were on the Pt island as well as on the terrace.<sup>18</sup> On the other hand, the stripe structure has still remained unchanged at the right part of Figure 4(b), indicating that the structure change has not yet occurred on the bare surface as well.

**Comparison between CO and NO adsorption.** Some important similarities between the interactions of CO and NO with a Pt(001) surface are observed during adsorption of molecules. At 90 K, both molecules are preferentially adsorbed on the surface Pt atoms having relatively lower coordination number. And then, domains of the adsorbates are rapidly grown on the reconstructed surface parallel to the  $[14\ 1]$  direction with lower migration energy.<sup>1,4,23,24</sup> Finally, the extra Pt atoms that were formed due to adsorbate-induced restructuring give rise to anisotropic islands on the ( $1 \times 1$ ) surface.

However, there is a remarkable difference between CO and NO adsorption. Only NO molecule (Figure 4(a)) was atomically visible as compared with CO molecule (Figure 1 and the region (II) of Figure 2(a)) under low coverages at 90 K. Since the value of barrier to CO diffusion (0.2 eV)<sup>27,28</sup> on Pt(111) is approximately equal to or larger than NO diffusion (0.14 eV),<sup>29</sup> this fact probably means that an interaction between adsorbates rather than between an adsorbate and a substrate plays an important role in explaining the different behaviors. We tentatively assume that the intermolecular interactions between NO-NO and between CO-CO are attractive and repulsive, respectively. Once a single adsorbed, movable NO molecule migrates and is trapped by an NO cluster, migration-depressed NO cluster is atomically visible during STM observation.

The different behavior on the STM images certainly originates from the intermolecular interactions. The interaction between CO molecules on a Pt(001) surface was calculated to be repulsive at a coverage of 0.5.<sup>9</sup> Similarly, pure repulsive interaction potential was reported by means of a Monte Carlo simulation for CO/Pt(111).<sup>30</sup> As for CO, therefore, the type of the interaction is good agreement with the previous studies.<sup>9,30</sup> On the other hand, it was reported that the interaction for NO on Pt(001) is calculated to be considerably stronger repulsive than that for CO/Pt(001).<sup>9</sup> A saturation coverage (showing  $c(4 \times 2)$  LEED pattern) used in the calculation is 0.5, twice as high as that measured very recent our STM image.<sup>18</sup> Therefore, the calculation result might not be suitable to the case of a coverage of 0.25. Also, a previous TDS study<sup>15</sup> that a desorption peak of NO from Pt(001) shifts from 470 K to 550 K with increasing coverage gives a strong evidence to support our assumption that NO-NO intermolecular interaction is attractive.

## References

- Linderoth, T. R.; Mortensen, J. J.; Jacobsen, K. W.; Lægsgaard, E.; Stensgaard, I.; Besenbacher, F. *Phys. Rev. Lett.* **1996**, *77*, 87.
- Borg, A.; Hilmen, A.-M.; Bergene, E. *Surf. Sci.* **1996**, *306*, 10.
- Song, M.-B.; Yoshimi, K.; Ito, M. *Chem. Phys. Lett.* **1996**, *263*, 585.
- Mase, K.; Murata, Y. *Surf. Sci.* **1991**, *242*, 132; **1992**, *277*, 97.
- Behm, R. J.; Thiel, P. A.; Norton, P. R.; Ertl, G. *J. Chem. Phys.* **1983**, *78*, 7437.
- Jackman, T. E.; Griffiths, K.; Davies, J. A.; Norton, P. R. *J. Chem. Phys.* **1983**, *79*, 3529.
- Hösler, W.; Ritter, E.; Behm, R. J. *Ber. Bunsenges. Phys. Chem.* **1986**, *90*, 205.
- Martin, R.; Gardner, P.; Bradshaw, A. M. *Surf. Sci.* **1995**, *342*, 69.
- Yeo, Y. Y.; Vattuone, L.; King, D. A. *J. Chem. Phys.* **1996**, *104*, 3810.
- Hopkinson, A.; Bradley, J. M.; Guo, X.-C.; King, D. A. *Phys. Rev. Lett.* **1993**, *71*, 1597.
- Vítus, C. M.; Chang, S.-C.; Schardt, B. C.; Weaver, M. J. *J. Phys. Chem.* **1991**, *95*, 7559.
- Bonzel, H. P.; Brodén, G.; Pirug, G. *J. Catal.* **1978**, *53*, 96.
- Gardner, P.; Martin, R.; Tüshaus, M.; Bradshaw, A. M. *Surf. Sci.* **1992**, *269/270*, 405.
- Brandt, M.; Zagatta, G.; Böwering, N.; Heinzmann, U. *Surf. Sci.* **1997**, *385*, 346.
- Lesley, M. W.; Schmidt, L. D. *Surf. Sci.* **1985**, *155*, 215.
- Ritter, E.; Behm, R. J.; Pötschke, G.; Wintterlin, J. *Surf. Sci.* **1987**, *181*, 403.
- Gardner, P.; Tüshaus, M.; Martin, R.; Bradshaw, A. M. *Surf. Sci.* **1990**, *240*, 112; *Vacuum* **1990**, *41*, 304.
- Song, M.-B.; Momoi, K.; Ito, M. *Jpn. J. Appl. Phys.* **1997**, *36*, L1528.
- Gorte, R. J.; Schmidt, L. D.; Gland, J. L. *Surf. Sci.* **1981**, *109*, 367.
- Schmid, M.; Biedermann, A.; Böhmig, S. D.; Weigand, P.; Varga, P. *Surf. Sci.* **1994**, *318*, 289.
- Murray, S. J.; Finetti, P.; Leible, F. M.; Diehl, R. D.; McGrath, R. *Chem. Phys. Lett.* **1995**, *237*, 474.
- Dunphy, J. C.; McIntyre, B. J.; Gomez, J.; Ogletree, D. F.; Somorjai, G. A.; Salmeron, M. B. *J. Chem. Phys.* **1994**, *100*, 6092.
- Günther, S.; Kopatzki, E.; Bartelt, M. C.; Evans, J. W.; Behm, R. J. *Phys. Rev. Lett.* **1994**, *73*, 553.
- Venik, H. J.; Berg, C.; Borg, A.; Raaen, S. *Phys. Rev.* **1996**, *B53*, 16587.
- Wandelt, K.; Markert, K.; Dolle, P.; Jablonski, A.; Niemantsverdriet, J. W. *Surf. Sci.* **1987**, *189/190*, 114.
- Hayden, B. E. *Surf. Sci.* **1983**, *131*, 419.
- Croci, M.; Felix, C.; Vandoni, G.; Harbich, W.; Monot, R. *Surf. Sci.* **1993**, *290*, L667.
- Hähner, G.; Toennies, J. P.; Wöll, C. *Appl. Phys.* **1990**, *A51*, 208.
- Lahaye, R. J. W. E.; Stolte, S.; Holloway, S.; Kleyn, A. W. *J. Phys. Chem.* **1996**, *104*, 8301.
- Persson, B. N. J.; Tüshaus, M.; Bradshaw, A. M. *J. Chem. Phys.* **1990**, *92*, 5034.